Prepared for submission to JINST

arXiv:2107.10207v2 [physics.ins-det] 1 Oct 2021

On the Use of Neural Networks for Energy Reconstruction in High-granularity Calorimeters

N. Akchurin, C. Cowden, J. Damgov, A. Hussain, and S. Kunori

Texas Tech University, Department of Physics and Astronomy,
Advanced Particle Detector Laboratory
Lubbock, TX, 79409, USA

Abstract: We studied the performance of the Convolutional Neural Network (CNN) for energy regression in a finely 3D-segmented calorimeter simulated by GEANT4. A CNN trained solely on a pure sample of pions achieved substantial improvement in the energy resolution for both single pions and jets over the conventional approaches. It maintained good performance for electron and photon reconstruction. We also used the Graph Neural Network (GNN) with edge convolution to assess the importance of timing information in the shower development for improved energy reconstruction. In this paper, we present the comparison of several reconstruction techniques: a simple energy sum, a dual-readout analog, a CNN, and a GNN with timing information.

Keywords: Calorimetry, high-granularity, dual-readout, multi-readout

Contents

1 Introduction **2**

2 Simulation Study **3**

3 Benchmark Energy Reconstruction Methodology **3**

4 CNN Energy Reconstruction Methodology **3**

5 CNN Performance with Single Hadron and Jets **6**

6 Reconstruction of f_{em} with CNN **8**

7 Beyond the f_{em} correction **8**

8 Using Timing Information with Graph Neural Networks (GNN) **9**

9 Remarks **10**

10 Acknowledgements **12**

1 Introduction

Calorimeters have played crucial roles in high energy physics experiments for decades. In the last two, new ideas and techniques, such as dual-readout [1] and particle flow [2, 3], emerged and contributed to the increased understanding of calorimeter fundamentals. Future accelerators, such as the high luminosity LHC or the FCC, push energy and luminosity bounds beyond our capacity today. We must design calorimeters with increased granularity, fast timing, and high degrees of radiation tolerance to perform at future accelerators.

Those involved in calorimeter design have known for some time that devices often exhibit different characteristic responses to different particle types. For instance, the different responses to electromagnetic and hadronic initiating particles, whose ratio is usually denoted as e/h, has led to many arguments to the merits of compensating ($e/h = 1$) *vs* non-compensating ($e/h \neq 1$) calorimeter designs. Since showers initiated by hadrons contain both electromagnetic (EM) and hadronic components, the fluctuation of the fraction of the initial energy into the EM component (f_{em}) drives much of the observed variance of the energy measurement. This insight, for instance, served as the impetus for the dual readout methodology in which a calorimeter with two readout types - with two different e/h ratios - allows experimenters to determine f_{em} on an event-by-event basis. One can measure energy much more precisely knowing f_{em} than not. However, other less significant response fractions still exist; for example, the fraction of the initial energy going undetected in inelastic nuclear interactions. Capturing these additional sources of fluctuations would require additional capabilities.

Interestingly, processes involved in the shower of particles inside a calorimeter have corresponding distributions of deposited energy. Experimentalists have overlooked this fact since previous calorimeters lack the spatial granularity to warrant the development of reconstruction algorithms so finely attuned to local regions of showers. The shear complexity of a reconstruction algorithm which could take advantage of such high granularity has also impeded much progress in this approach.

Recently the CMS experiment has adopted a high granularity calorimeter design as part of its end-cap upgrade [4]. This has prompted further developments in reconstruction techniques which employ advanced pattern recognition techniques such as image processing.

The advance of the Convolutional Neural Network (CNN) [5, 6], and neural networks in general, can allow us to more elegantly solve this challenging problem of reconstruction. We can take advantage of the CNN's sensitivity to spatially distributed signals to develop a model that accurately estimates the initiating particle's energy from a high granularity calorimeter. Graph Neural Networks (GNN) [7] may potentially have advantages over the CNN since the GNN can accommodate a variety of geometry that a CNN cannot. This detail implies that a GNN may be better suited to a full size experimental detector geometry. In fact, many researchers have already studied applications of these techniques in the context of HEP collider experiments. The application of CNNs were been tested in simulation for energy reconstruction on single pions [8, 9] as well more general detector settings [10]. Several studies have investigated GNNs for the clustering as part of the particle flow application with multiple pions [11–14]. Another study investigated the separation between neutral and charged hadrons depositions within the same calorimeter volume [15]. We also note, that neural networks have been successfully applied for particle identification [9, 16]. We do not intend for this serve as an exhaustive list related studies,

but our intention is to relate to a broader and increasing documented area of study.

We studied in detail the performance of a CNN applied to energy regression in a finely 3D-segmented calorimeter simulation. We also introduce a GNN into this study to evaluate the contribution of precise timing to energy reconstruction performance. In our investigation of energy reconstruction using these techniques, we see promising improvements in resolution beyond what has been demonstrated by dual, and proposed triple, readout calorimeters [17]. We intend to use these investigations as a stepping stone in the development of state-of-the-art calorimeters for future experiments. Comparison of neural network architectures and their application to the particle flow algorithm remains outside of the scope of this study.

In the next sections, we shall describe our simulation study and the reconstruction methods that we examined. In Section 5, we describe the resulting performance. We describe the estimation of f_{em} with a CNN in Section 6, and we describe a further study showing the CNN's ability to leverage topological information to improve resolution in a compensating calorimeter in Section 7. In Section 8, we introduce timing information and reconstruct energy with a GNN.

2 Simulation Study

We simulated a sampling calorimeter with alternating plates of 17 mm copper (absorber) and 3 mm silicon (active material) with GEANT4 [18] version 4.10.06 and we used the FTFP_BERT physics list to describe the hadronic interactions. The calorimeter is 1.5 m deep (8.8 interaction lengths) and covers $1{\times}1$ m^2 in transverse direction. The volume is divided in $2 \times 2 \times 2$ cm^3 cells, representing individual readout channels. The minimum ionizing particle (MIP) signal is about 1.0 MeV per cell and we set the minimum energy threshold at 0.6 MeV/cell in this study. Electronics noise is not taken into account. The position of incident particles is smeared in a 4×4 cm^2 in transverse plane.

3 Benchmark Energy Reconstruction Methodology

We used two traditional energy reconstruction techniques to benchmark performance of current methods. The first and simplest approach is the linear sum of all deposited energy where the active material is calibrated using electrons. In the second technique, we employ to benchmark the potential performance of a comparable dual-readout calorimeter. In it, we exploited information from the GEANT4 simulation to correct the energy sum for the f_{em} of the shower.

Figure 1 shows the responses of the simple and f_{em} corrected energy sum reconstruction techniques on a sample pion initiated showers. We can see that the f_{em} corrected energy sum largely restores the response linearity, as one expects from dual-readout.

4 CNN Energy Reconstruction Methodology

Complexity of the hadronic shower poses serious challenges to the analysis techniques targeting energy reconstruction based on the distribution of energy deposited throughout the calorimeter volume.

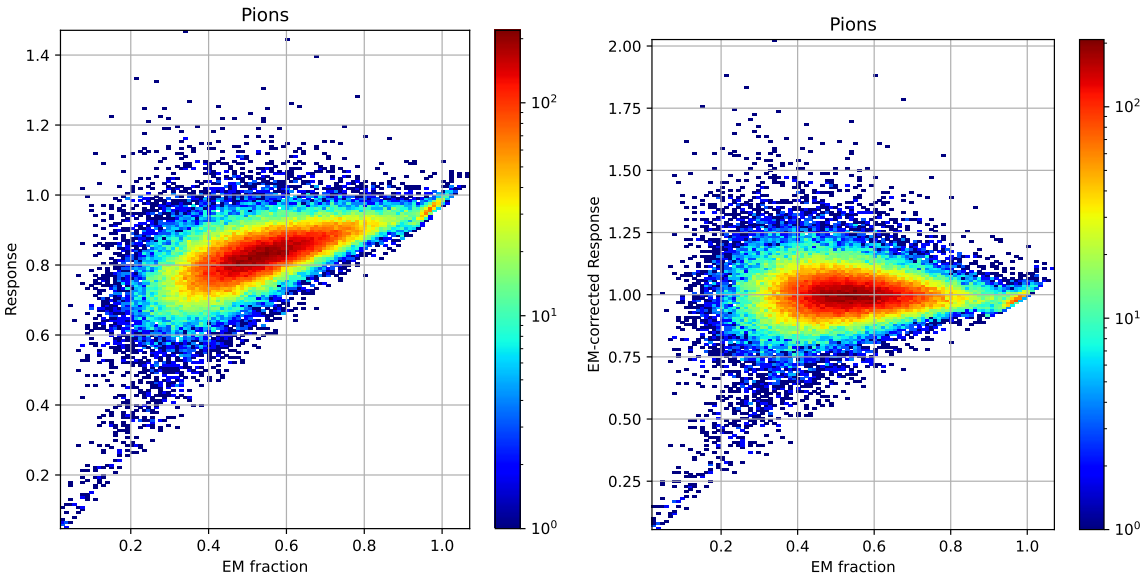

Figure 1. The calorimeter response: simple energy sum over all channels (left) and f_{em} corrected energy sum (right) for pions with energy from 5 to 150 GeV. Entries with low EM and low response are from events with low showering activity and MIP-like tracks in the calorimeter volume.

The nuclear interactions involved in hadronic showers open up many more possible signal generating processes compared to electromagnetic showers.

Hadronic showers have complex correlation and dependencies amongst the observed signals because the various particle species emerging from a particular nuclear interaction subsequently deposit energy and participate in processes characteristic of the species. For instance, the invisible energy in the hadron component is strongly associated with the multiplicity of secondary charged hadrons as one can see in Figure 2. The distribution shown in Figure 2 does not appear as a simple correlation between the two variables; the distribution appears to have multiple modes and correlated strata which indicates we need some other variable or variables to fully explain this distribution. This is only one example of one pair of shower attributes.

There are two main groups of secondaries with distinct topological properties. The first group encompasses secondaries from intra-nuclear scattering - mainly light mesons (*i.e.* pions) which have a small deflection angle with respect to the direction of the initial hadron. The second group consists of the product of nuclear de-excitation; its predominant contribution comes the from protons and neutrons emitted at significantly large angles. High granularity calorimeters offer unique opportunities to detect topological signatures, such as tracks of the charged hadrons, and extract information to estimate, or compensate, for the undetected invisible energy.

The common coincidence and overlap of the various topological signals, for instance EM showers often overlap the tracks from charged hadrons, makes it difficult to efficiently reconstruct the event with traditional techniques.

The array of cell responses of a highly granular calorimeter resembles a 3D image to which CNNs

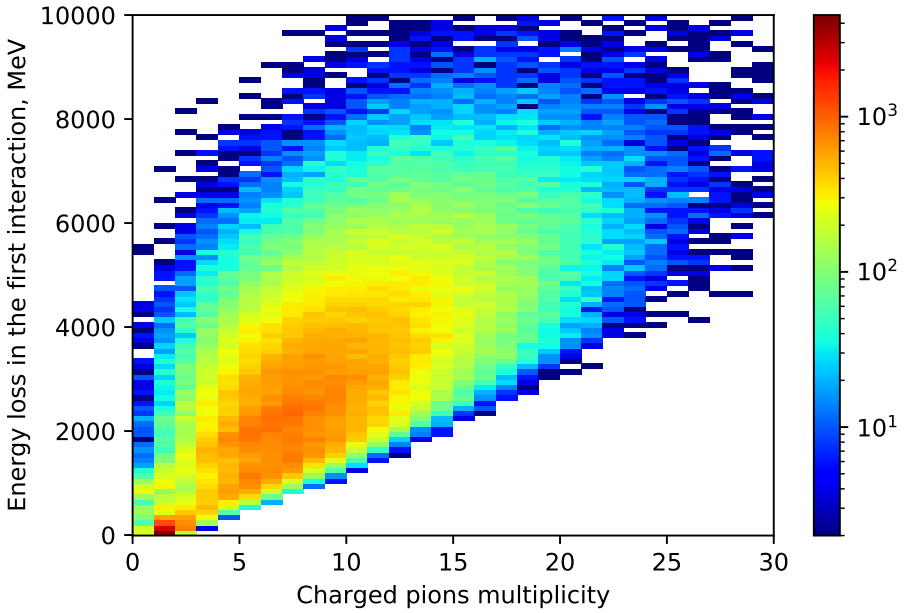

Figure 2. Energy loss at the first interaction is strongly correlated with the charged pion multiplicity in the hadronic showers as predicted by GEANT4. Such relations between the invisible energy and specific features of the visible signal are utilized by neural networks for improved energy reconstruction.

are well suited to extract high level properties of the objects found within.

We can treat the energy deposition in such a calorimeter as approximating a mono-chrome 3D image where the deposited energy represents the brightness level. The input image is a $50 \times 50 \times 75$ array of energy measurements. The CNN in this analysis consists of 3D convolutional, max pooling, and flattened and dense layers as shown in Figure 3. The energy sum is represented as an additional input node in the flattened layer, which forces the CNN to work in energy correction regime and results in better overall response linearity.

We optimize the mean square logarithmic error to estimate the model parameters to achieve more balanced contributions from low and high energies. The Adam optimization algorithm [19] is used with early stopping based on the validation loss. Regularization in the training process is implemented with `BatchNormalization` layer [20] and `DropOut`(0.2) [21] in the dense layers. In this configuration, the CNN energy reconstruction effectively works as an energy correction to the raw energy sum. Correcting the raw energy sum allows the CNN to apply more universally to energy reconstruction of different particle types and multiplicities. For example, the CNN derived energy correction in photon-initiated showers is negligible; the reconstruction performance is very similar to that of the simple energy sum since EM showers have few hadronic secondaries in the shower.

In the case of jets, the performance is expected to be similar to single-particle performance as the invisible energy in the particular hadronic interaction depends only on the initiating hadron and the media properties.

Studies based on Class Activation Mapping [22] revealed that energy correction is mostly derived

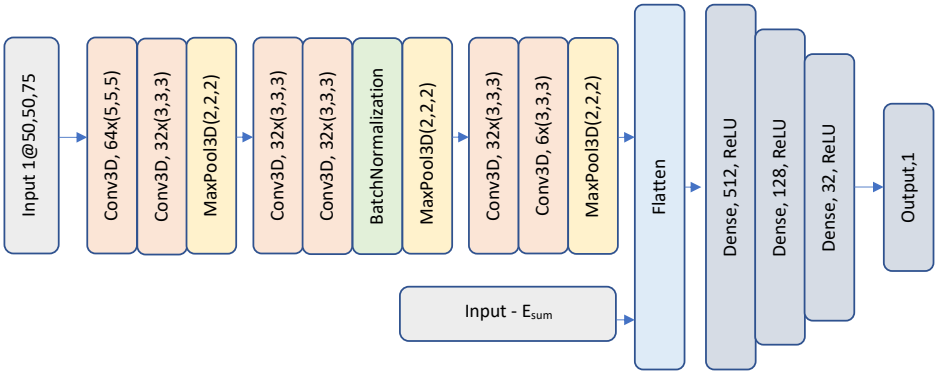

Figure 3. The CNN architecture consists of several alternating 3D Convolutional and MaxPooling layers in this work. Energy sum over the active volume is represented as an additional node in the flattened layer. Three Dense layer with Dropout(0.2) are used.

by the CNN in regions near individual hadron interactions with traces from charged hadrons and just outside regions of substantial EM energy depositions. These regions contain representative information on the multiplicity and production angle of the secondary charged hadrons. These studies give us insight into how the CNN infers the undetected, invisible energy from the available visible signals.

5 CNN Performance with Single Hadron and Jets

The 3D CNN is trained on a GEANT4-simulated data set with 0.5 to 150 GeV charged pions. The energy reconstruction performance is then tested on an independent sample in the same energy range. Figure 4 shows the reconstruction performance of the CNN compared against the simple energy sum and dual-readout approach. We have included parametric energy resolution fits of the form $\frac{a}{\sqrt{E}} + b$ where a and b represent the stochastic and constant terms to the comparison plots. One can see that the CNN outperforms both alternative reconstruction methodologies. Here, the f_{em} correction method represents a dual-readout approach where f_{em} is computed from the energy deposited by the electrons in the shower.

The CNN performance on electrons is illustrated in Figure 5; again the figure illustrates the performance of the simple sum for comparison. We see the CNN performance closely resembles, with minimal degradation, the performance of the simmple energy sum. By the design of our CNN architecture we anticipated the similar performance because the CNN operates as an energy correction.

Thus, in the case of showers initiated by photons or electrons, the CNN does not find traces from charged hadrons and the correction to the raw calorimeter response is negligible. As a result, a CNN trained with pion data sets can reconstruct electron/photon energy without introducing a strong, undesired bias. We did not study the performance of a CNN trained on a population comprised of pions and electrons.

We further examined the CNN reconstruction performance on jets by using PYTHIA8 [23] to simulate u-quark jets with energy from 20 GeV to 1 TeV. The response linearity and energy resolution

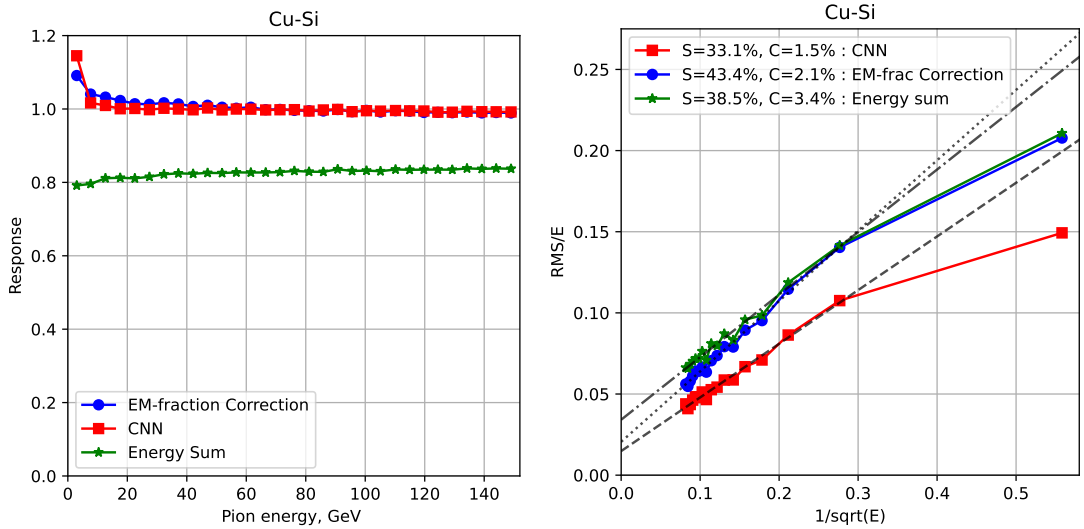

Figure 4. The calorimeter response (left) and energy resolution (right) for charged pions are shown. The simple sum over all channels (green), with the f_{em} correction (red) and the CNN regression (blue) show respective energy measurement performance. The energy resolution parameters representing stochastic (S) and constant (C) effects estimated by a linear fit are included in the legend.

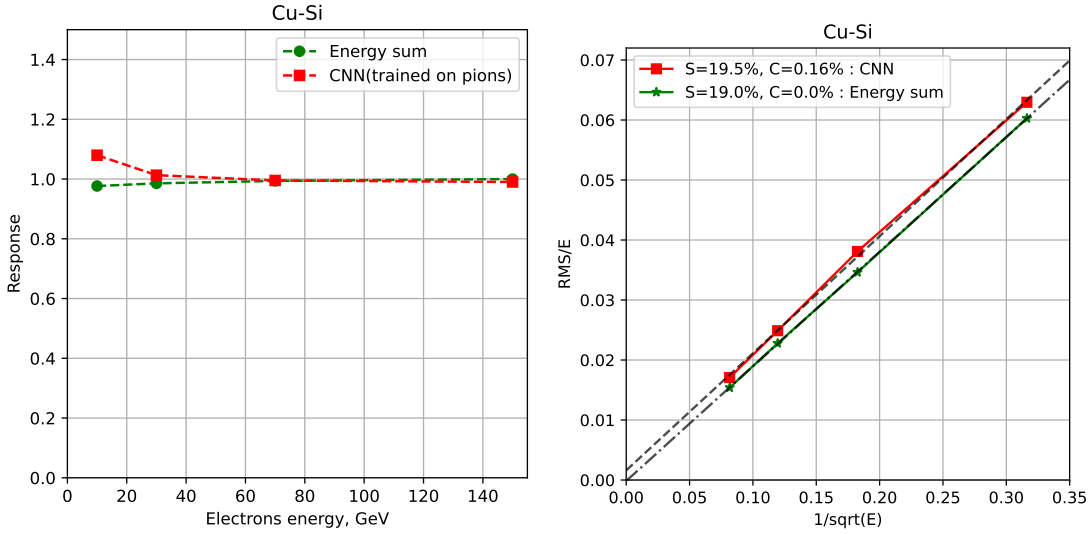

Figure 5. The calorimeter response (left) and energy resolution (right) for electrons: the sum over all channels (green) and the CNN regression (red) result in similar performance for a CNN that has been trained on pions alone.

is shown in Figure 6. The energy scale is preserved without the need for additional corrections. The energy resolution is also significantly improved when compared to the more traditional reconstruction techniques.

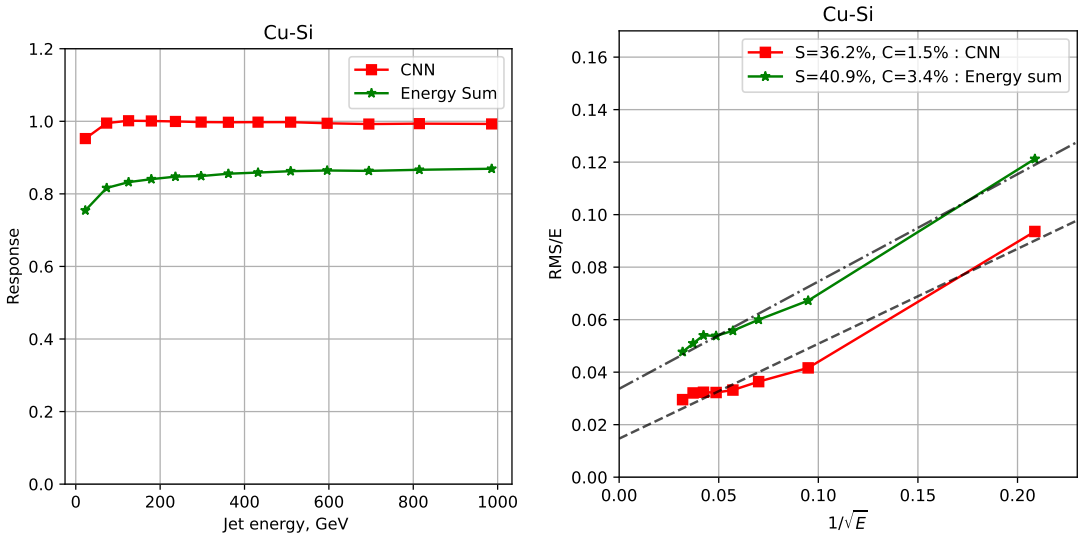

Figure 6. The response (left) and energy resolution (right) for jets: the sum over all channels (green) and CNN regression (red).

6 Reconstruction of f_{em} with CNN

The large fluctuations in f_{em} in non-compensating calorimeters is the leading source for performance degradation in energy reconstruction. Dual-readout calorimeters are designed to infer f_{em} on an event-by-event basis by using signals from scintillation and Cherenkov light. We have tested an alternative approach for f_{em} reconstruction in a single-readout calorimeter using a CNN that leverages topological information in the shower development. The CNN is trained on simulated charged pions 0.5-150 GeV to reconstruct f_{em} and f_{had}.

Figure 7 shows the simulated f_{em} (left) and the ratio of the reconstructed to simulated f_{em} (right) over the range of imitating particle energies. One can deduce the viability of reconstructing f_{em} in a single readout high granularity calorimeter from the result illustrated in this figure.

7 Beyond the f_{em} correction

We also studied the energy reconstruction using a compensating ($e/h = 1$) calorimeter where the f_{em} fluctuations are no longer the leading cause for degraded performance.

The simulated U-Si calorimeter shows linear response to pions using simple sum for energy reconstruction. The improved reconstruction performance of the CNN over the simple energy sum as shown in Figure 8 indicates that the CNN exploits the relationship between the invisible energy and the visible signal in the shower, *i.e.* the multiplicity and production angle of the secondaries from the hadron interactions.

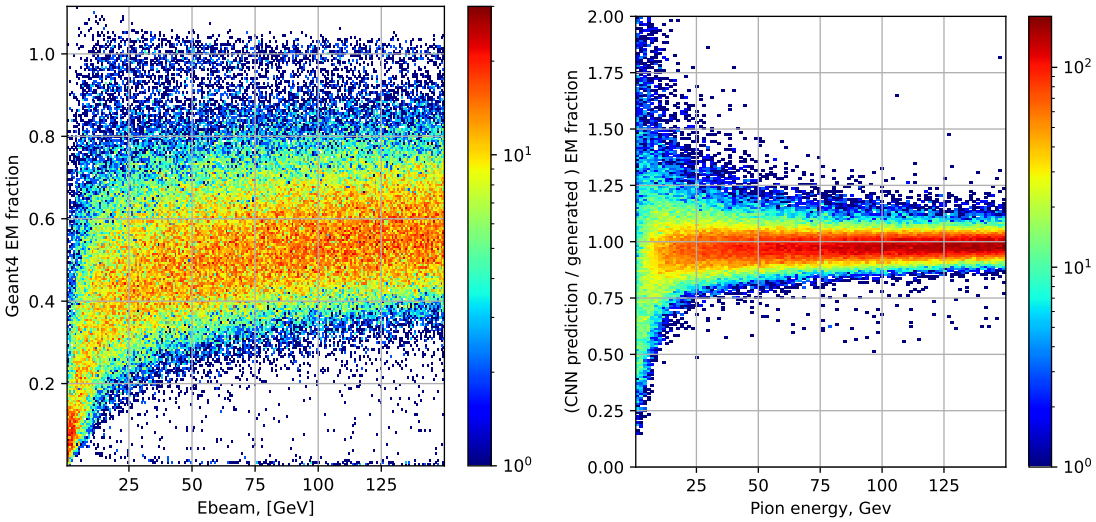

Figure 7. The electromagnetic fraction in the energy deposit by pions (left) and the predicted EM fraction by the CNN normalized to the true value (right).

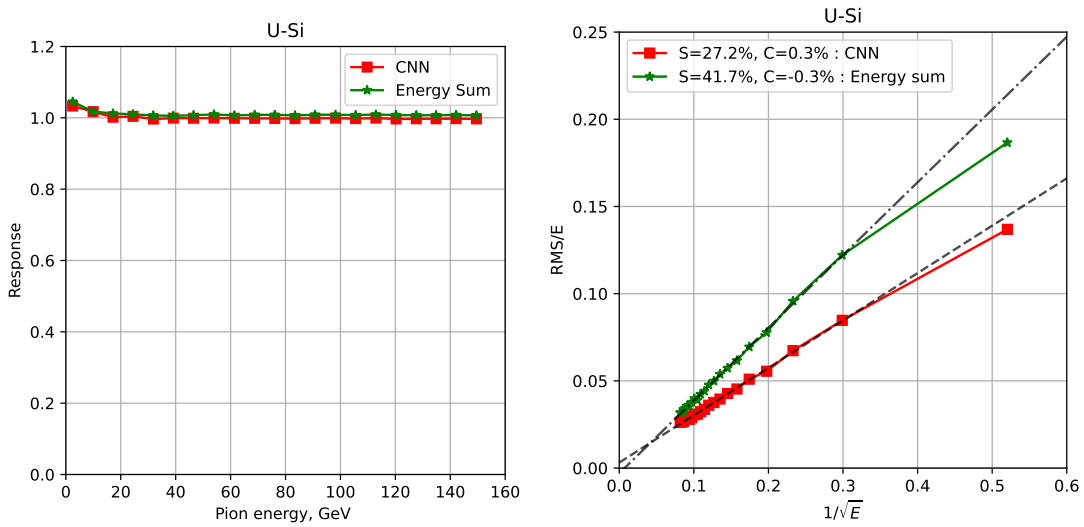

Figure 8. The response (left) and energy resolution (right) for pions: the sum over all channels (green) CNN regression(red).

8 Using Timing Information with Graph Neural Networks (GNN)

Graph Neural Networks (GNNs) can cope with irregular detector geometries which make them potential candidates for use in a full-size collider based experiment. Further, GNNs allow for the assignment of an arbitrary number of properties to a cell, thereby allowing us to easily incorporate multi-readout and timing information. We chose a GNN with edge convolution, like Dynamic Graph CNN [24, 25] to investigate the impact of precise timing for energy reconstruction. We studied the GNN performance

on the same Cu/Si setup described above.

Single pion and electron event energy distributions in space for various integration times[1] are shown respectively in Figures 9 and 10.

Each subfigure gives a representation of the spatial distribution of energy at some integration time; the y-axis represents the radial distance from the shower axis and the x-axis represents the longitudinal depth of the shower. We chose this form of visualization to draw attention to the development of the radial extent of showers at different time scales.

Unlike hadron showers, the electron initiated energy depositions take place promptly without much structure; low energy photons form the energy deposits found deep or transversely far from the shower axis in the calorimeter. Roughly speaking, by going from long to short integration times, we effectively transversely segment this calorimeter. This segmentation supplies important information since the time scales of some hadronic processes are much longer than the EM processes.

Figure 11 illustrates the effect of increasingly better timing measurement on energy resolution. Each data point (solid and open circles) includes several time slices. While the signal is integrated for 10 ns for all data points, the precision with which timing intervals are known is plotted on the horizontal axis. For example, the timing precision of 0.5 ns includes time intervals (0-0.5 ns), (0, 4 ns), (0, 1 ns) and (0, 0.5 ns) and plotted at 0.5 ns. As shorter time slices are included, the energy resolution improved somewhat for the two cases (30 and 100 GeV pions) we analyzed. We posit that information inherent in short time slices, possibly due to low energy protons, contribute additional information to the network. Essentially, protons in shorter time scales seem to stand in for neutrons in longer time scales for enhanced energy measurement.

The GNN selects the local region of interest by a fixed number of cells with non-zero energy (k Nearest Neighbours). The size of the region varies with the density of the active cells, which is also correlated with the energy of the incident particle. In contrast the CNN, it uses a fixed size for the local region of interest defined by the filter size. This leads to the observed difference in the performance between CNN and GNN as function of the particle energy and is subject of further development and tuning of these algorithms. In this study, we mostly focused on exploring possible improvement in energy reconstruction by the addition shower timing information.

9 Remarks

In conclusion, we have observed enticing performance results from our simulation study of advanced energy reconstruction methodologies applied to a high granularity calorimeter module. The CNN response to pions appears quite linear at high energies, it tends towards unity faster than the simpler method based on $f_{\rm em}$, and it also significantly outperforms both the energy sum and $f_{\rm em}$ methods in terms of energy resolution. By regressing, *e.g.* estimating, $f_{\rm em}$ and $f_{\rm had}$ with a CNN model we add further support to our deduction that the evidence of these fluctuations exists within the spatial distribution of deposited energy. Similarly, the improved energy resolution noted in the study of a compensating ($e/h = 1$), U-Si module suggests the CNN's sensitivity to $f_{\rm had}$. Altogether, this

[1]We denote the duration of the window of time a signal may be collected and observed as the integration time.

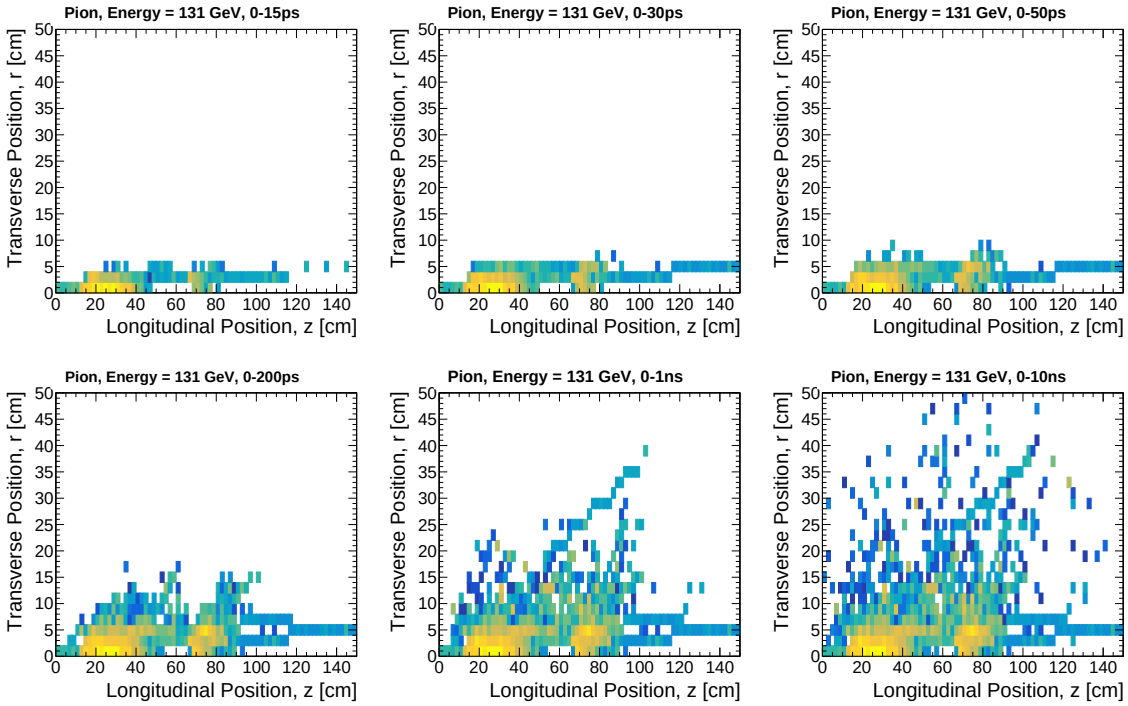

Figure 9. The energy deposits due to a single 131 GeV charged pion are shown in $r-z$ coordinates where the colors indicate deposited energy. As indicated on top of each each plot, the integration times gradually increase from 0-15 ps (top left) to 0-10 ns (bottom right). Time is 'local', in other words, it is corrected for the travel time, $t_l = t - z/c$, along z-axis for all particles.

evidence suggests that the CNN/GNN methodology applied in high granularity calorimeters surpasses the hadronic energy resolution attainable with a comparable dual-readout device. Finally, we studied the prospects of a GNN applied to our simulated calorimeter module with the addition of precision timing information. We observed a time precision dependence of energy resolution - better timing, better resolution - roughly comparable to that of the CNN. The GNN's energy resolution surpasses the CNN's below ~ 100 ps.

We have shown clear performance benefits by application of advance energy reconstruction techniques in a high granularity calorimeter. We have also seen evidence which suggests that the neural network type reconstruction models take advantage of the spatial, and spatial-temporal, distribution of deposited energy to realize such gains. Although the precise way in which the CNN accounts for $f_{\rm em}$ and $f_{\rm had}$ remains unknown, we have shown that the CNN's sensitivity by showing that it can estimate these fractions based on the energy distributions. This observation carries important implications for multi-readout calorimetry since the capability to estimate $f_{\rm em}$ and $f_{\rm had}$ from a single readout device may be at hand.

Future studies will quantify the performance gains sustained when the simulation includes electronic noise, intercalibration, and other issues which impact physical devices. One may pessimistically anticipate the CNN performance to degrade as noise increases and input response becomes less ho-

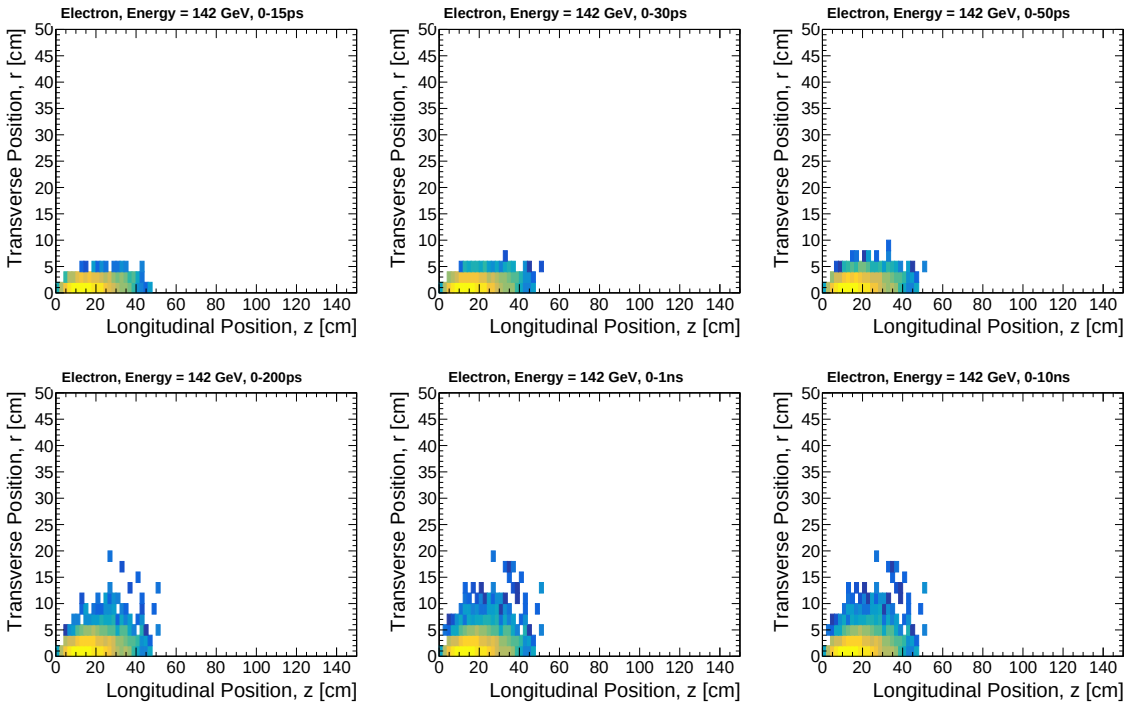

Figure 10. The energy deposits due to a single 142 GeV electron are shown in $r - z$ coordinates where the colors indicate deposited energy. As indicated on top of each each plot, the integration times gradually increase from 0-15 ps (top left) to 0-10 ns (bottom right). Time is 'local', in other words, it is corrected for the travel time, $t_l = t - z/c$, along z-axis for all particles.

mogeneous; however, we have seen such comfortable margin of improvement over the simple energy sum and dual readout analog that we can still expect some good degree of improvement.

10 Acknowledgements

This work has been supported by the US Department of Energy, Office of Science (DE-SC001592) and Texas Tech University, Office of the Vice President for Research and Innovation.

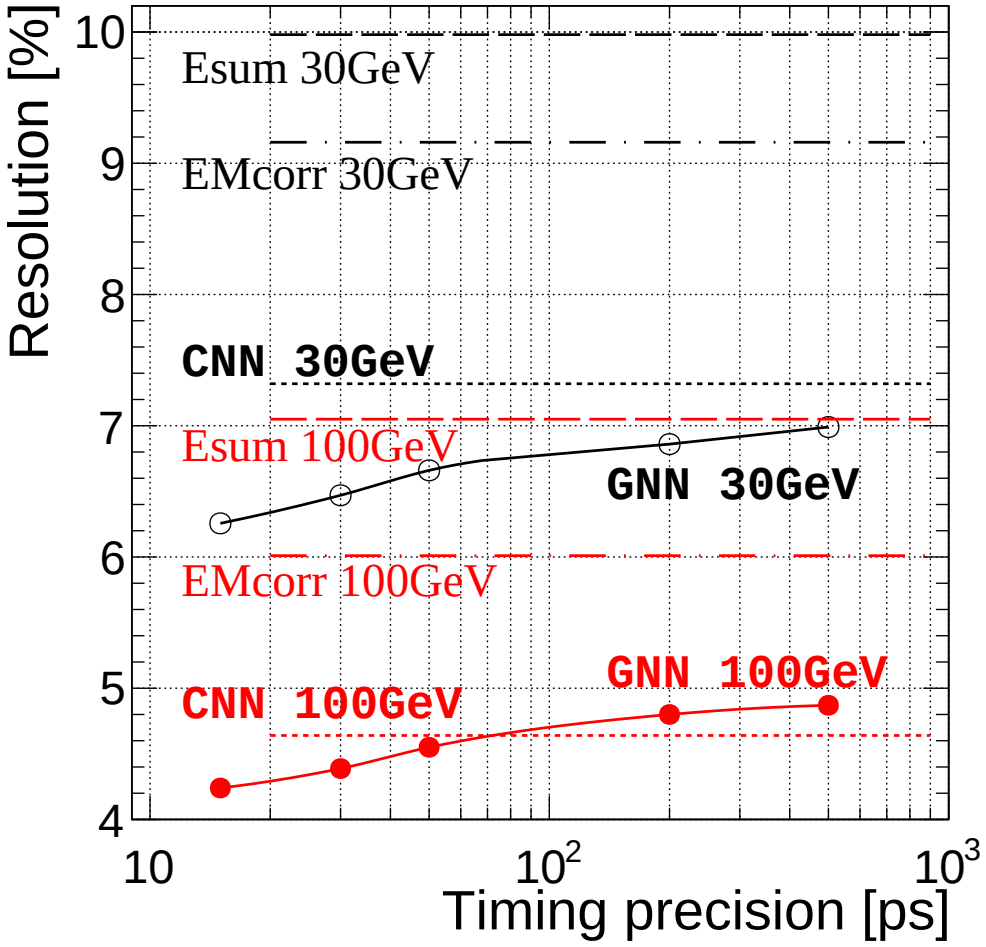

Figure 11. The energy resolution (σ/E) for 30 GeV (black) and 100 GeV (red) pions. Simple energy sum (Esum), f_{em} corrected energy sum (EMcorr), CNN and GNN reconstruction techniques. The horizontal axis indicates the assumed timing precision for the GNN technique. The energy resolutions obtained from different reconstruction techniques are also shown for comparison.

References

[1] N. Akchurin, K. Carrell, J. Hauptman, H. Kim, H. Paar, A. Penzo, R. Thomas, R. Wigmans, Hadron and jet detection with a dual-readout calorimeter, Nuclear Instruments and Methods in Physics Research Section A: Accelerators, Spectrometers, Detectors and Associated Equipment 537 (3) (2005) 537–561. doi:https://doi.org/10.1016/j.nima.2004.07.285.
URL https://www.sciencedirect.com/science/article/pii/S0168900204018091

[2] F. Sefkow, A. White, K. Kawagoe, R. Pöschl, J. Repond, Experimental Tests of Particle Flow Calorimetry, Rev. Mod. Phys. 88 (2016) 015003. arXiv:1507.05893, doi:10.1103/RevModPhys.88.015003.

[3] The CMS Collaboration, Particle-flow reconstruction and global event description with the CMS detector, Journal of Instrumentation 12 (10) (2017) P10003–P10003.

doi:10.1088/1748-0221/12/10/p10003.
URL https://doi.org/10.1088/1748-0221/12/10/p10003

[4] CMSCollaboration, The Phase-2 Upgrade of the CMS Endcap Calorimeter, Tech. Rep. CERN-LHCC-2017-023. CMS-TDR-019, CERN, Geneva, technical Design Report of the endcap calorimeter for the Phase-2 upgrade of the CMS experiment, in view of the HL-LHC run. (Nov 2017).
URL https://cds.cern.ch/record/2293646

[5] K. Fukushima, Neural network model for a mechanism of pattern recognition unaffected by shift in position - neocognitron, Trans. IECE J62-A(10):658–665.

[6] Y. LeCun, Y. Bengio, G. Hinton, Deep learning, Nature 521 (7553) (2015) 436–444.
doi:10.1038/nature14539.
URL https://doi.org/10.1038/nature14539

[7] Z. Wu, S. Pan, F. Chen, G. Long, C. Zhang, P. S. Yu, A comprehensive survey on graph neural networks, IEEE Transactions on Neural Networks and Learning Systems 32 (1) (2021) 4–24.
doi:10.1109/TNNLS.2020.2978386.

[8] C. Neubüser, J. Kieseler, P. Lujan, Optimising longitudinal and lateral calorimeter granularity for software compensation in hadronic showers using deep neural networks (2021). arXiv:2101.08150.

[9] D. Belayneh, F. Carminati, A. Farbin, B. Hooberman, G. Khattak, M. Liu, J. Liu, D. Olivito, V. B. Pacela, M. Pierini, et al., Calorimetry with deep learning: particle simulation and reconstruction for collider physics, The European Physical Journal C 80 (7). doi:10.1140/epjc/s10052-020-8251-9.
URL http://dx.doi.org/10.1140/epjc/s10052-020-8251-9

[10] M. Aleksa, P. Allport, R. Bosley, J. Faltova, J. Gentil, R. Goncalo, C. Helsens, A. Henriques, A. Karyukhin, J. Kieseler, C. Neubüser, H. F. P. D. Silva, T. Price, J. Schliwinski, M. Selvaggi, O. Solovyanov, A. Zaborowska, Calorimeters for the fcc-hh (2019). arXiv:1912.09962.

[11] S. R. Qasim, J. Kieseler, Y. Iiyama, M. Pierini, Learning representations of irregular particle-detector geometry with distance-weighted graph networks, The European Physical Journal C 79 (7).
doi:10.1140/epjc/s10052-019-7113-9.
URL http://dx.doi.org/10.1140/epjc/s10052-019-7113-9

[12] J. Kieseler, Object condensation: one-stage grid-free multi-object reconstruction in physics detectors, graph, and image data, The European Physical Journal C 80 (9).
doi:10.1140/epjc/s10052-020-08461-2.
URL http://dx.doi.org/10.1140/epjc/s10052-020-08461-2

[13] S. R. Qasim, K. Long, J. Kieseler, M. Pierini, R. Nawaz, Multi-particle reconstruction in the high granularity calorimeter using object condensation and graph neural networks (2021).
arXiv:2106.01832.

[14] X. Ju, S. Farrell, P. Calafiura, D. Murnane, Prabhat, L. Gray, T. Klijnsma, K. Pedro, G. Cerati, J. Kowalkowski, G. Perdue, P. Spentzouris, N. Tran, J.-R. Vlimant, A. Zlokapa, J. Pata, M. Spiropulu, S. An, A. Aurisano, J. Hewes, A. Tsaris, K. Terao, T. Usher, Graph neural networks for particle reconstruction in high energy physics detectors (2020). arXiv:2003.11603.

[15] F. A. Di Bello, S. Ganguly, E. Gross, M. Kado, M. Pitt, L. Santi, J. Shlomi, Towards a computer vision particle flow, The European Physical Journal C 81 (2). doi:10.1140/epjc/s10052-021-08897-0.
URL http://dx.doi.org/10.1140/epjc/s10052-021-08897-0

[16] L. de Oliveira, B. Nachman, M. Paganini, Electromagnetic showers beyond shower shapes, Nuclear Instruments and Methods in Physics Research Section A: Accelerators, Spectrometers, Detectors and Associated Equipment 951 (2020) 162879. doi:10.1016/j.nima.2019.162879.
URL http://dx.doi.org/10.1016/j.nima.2019.162879

[17] D. E. Groom, Energy flow in a hadronic cascade: Application to hadron calorimetry, Nuclear Instruments and Methods in Physics Research Section A: Accelerators, Spectrometers, Detectors and Associated Equipment 572 (2) (2007) 633–653. doi:https://doi.org/10.1016/j.nima.2006.11.070.
URL https://www.sciencedirect.com/science/article/pii/S0168900206023965

[18] S. Agostinelli, et al., GEANT4–a simulation toolkit, Nucl. Instrum. Meth. A 506 (2003) 250–303. doi:10.1016/S0168-9002(03)01368-8.

[19] J. B. Diederik P. Kingma, Adam: A method for stochastic optimization (2014). arXiv:1412.6980.

[20] S. Ioffe, C. Szegedy, Batch normalization: Accelerating deep network training by reducing internal covariate shift, CoRR abs/1502.03167. arXiv:1502.03167.
URL http://arxiv.org/abs/1502.03167

[21] N. Srivastava, G. E. Hinton, A. Krizhevsky, I. Sutskever, R. Salakhutdinov, Dropout: a simple way to prevent neural networks from overfitting., Journal of Machine Learning Research 15 (1) (2014) 1929–1958.
URL http://www.cs.toronto.edu/~rsalakhu/papers/srivastava14a.pdf

[22] M. D. Zeiler, R. Fergus, Visualizing and understanding convolutional networks (2013). arXiv:1311.2901.

[23] T. Sjöstrand, S. Ask, J. R. Christiansen, R. Corke, N. Desai, P. Ilten, S. Mrenna, S. Prestel, C. O. Rasmussen, P. Z. Skands, An Introduction to PYTHIA 8.2arXiv:1410.3012.
URL https://bib-pubdb1.desy.de/record/191756

[24] Y. Wang, Y. Sun, Z. Liu, S. Sarma, M. Bronstein, J. Solomon, Dynamic graph cnn for learning on point clouds, ACM TRANSACTIONS ON GRAPHICS 38. doi:10.1145/3326362.
URL http://dx.doi.org/10.1145/3326362

[25] H. Qu, L. Gouskos, Jet tagging via particle clouds, Physical Review D 101 (5). doi:10.1103/physrevd.101.056019.
URL http://dx.doi.org/10.1103/PhysRevD.101.056019